



CYCLIC PUSHOVER TEST ON AN UNREINFORCED MASONRY STRUCTURE RESEMBLING A TYPICAL DUTCH TERRACED HOUSE

R. Esposito⁽¹⁾, K.C. Terwel⁽²⁾, G.J.P. Ravenshorst⁽³⁾, H.R. Schipper⁽⁴⁾, F. Messali⁽⁵⁾ and J.G Rots⁽⁶⁾

⁽¹⁾ Postdoctoral researcher, Delft University of Technology, Section of Structural Mechanics, r.esposito@tudelft.nl

⁽²⁾ Assistant professor, Delft University of Technology, Section of Structural and Building Engineering, k.c.terwel@tudelft.nl

⁽³⁾ Assistant professor, Delft University of Technology, Section of Structural and Building Engineering, g.j.p.ravenshorst@tudelft.nl

⁽⁴⁾ Assistant professor, Delft University of Technology, Section of Structural and Building Engineering, h.r.schipper@tudelft.nl

⁽⁵⁾ Postdoctoral researcher, Delft University of Technology, Section of Structural Mechanics, f.messali@tudelft.nl

⁽⁶⁾ Full professor, Delft University of Technology, Section of Structural Mechanics, j.g.rots@tudelft.nl

Abstract

During the last years, induced seismicity in the northern part of the Netherlands increased and the seismic assessment of unreinforced masonry (URM) structures became an important issue. As the problem is recent, the current building stock is not designed to withstand earthquakes and national guidelines are under development, but currently not yet legally mandatory. Consequently, the validation of analysis methods, such as numerical models, for the assessment of URM buildings became of importance. In order to provide benchmarks for the validation procedures, an extensive experimental campaign was carried out at Delft University of Technology in 2015. The campaign selected as case study a terraced house typology, which was extensively built in the Netherlands during the period 1960-1980. The focus was on the characterisation of the typology at various levels: material, connection, component and assemblage level. In this paper, the experimental findings related to a cyclic pushover test on an assembled structure resembling a typical Dutch terraced house are presented.

Keywords: Unreinforced masonry structures; Experiments; Cyclic test: Pushover test; Structural response

1 Introduction

In recent years induced seismicity in the northern part of the Netherlands considerably increased. This phenomenon has a wide impact on the built environment, which is mainly composed of unreinforced masonry. These buildings were not designed for seismic loading, and have particular characteristics, such as very slender walls (100 mm thickness and 2.5 m in height), limited cooperation between walls and floors, and extensive use of cavity walls.

To assess the behaviour of these existing unreinforced masonry (URM) buildings, the use of numerical models as well as analytical design methods is required. Various approaches are usually adopted for this purpose considering various degrees of accuracy and of complexity.

The validation of the analysis methods should be performed against well-defined benchmarks. In literature various benchmarks can be found on the seismic behaviour of URM buildings. These laboratory tests can range from full-scale shaking table (e.g. Ref. [1]) or cyclic pushover tests (e.g. Ref. [2]-[3]) up to large-scale tests on single elements (e.g. Ref. [4]-[9]), such as in-plane or out-of-plane tests.

To provide benchmarks for the Dutch situation [10], an extensive testing campaign was performed at Delft University of Technology in 2015. The campaign selected as case study a terraced house typology, which was commonly built in the Netherlands during the period 1960-1980. This typology is characterised by slender cavity walls, concrete floors and a timber roof covered with roof tiles. Experimental tests were carried out at various scales in order to characterise the masonry material [11], the connection [11], the vulnerable elements [12]-[14] and the structural behaviour [15]. This experimental campaign was included in an integrated testing program, part of which was developed at the European Centre for Training and Research in Earthquake [16].

In this paper, the experimental findings related to the cyclic pushover tests are presented [15]. A detailed description of the specimen and of the test set-up is presented in Section 2. Sections 3 and 4 describe the material properties and the testing procedure, respectively. The experimental findings are presented in Section 5, while a qualitative analytical calculation is illustrated in Section 6. Section 7 reports the main concluding remarks.



2 Description of the test specimen

The test aims to assess the structural response of a typical Dutch terraced house built in the period 1960-1980. Although many differences can be found from building to building, similar aspects characterise this typology in the selected period. Terraced houses are usually composed of 5 to 10 housing units. Each of them is typically a two-story high masonry building. The units are characterised by a narrow floor plan being approximately 5 m in width and 7-9 m in depth. The interstorey height varies typically between 2.5 and 2.7 m. The construction is characterised by the presence of large daylight opening in the facades. Consequently, the loadbearing structure is composed of very slender piers and long transversal walls. The loadbearing walls are mainly cavity walls, which leaves are connected by steel ties. Different masonry type were used during the years including solid clay or calcium silicate brick masonry for the inner leaf and solid or perforated clay brick masonry for the outer leaf. The majority of the buildings present concrete floors, which can be cast in-situ or prefabricated. The transversal walls are loadbearing and carry the floors, while the piers in the facades do not. The floors can span over a single house or be continuing for more than a housing unit. The timber roofs are usually adopted

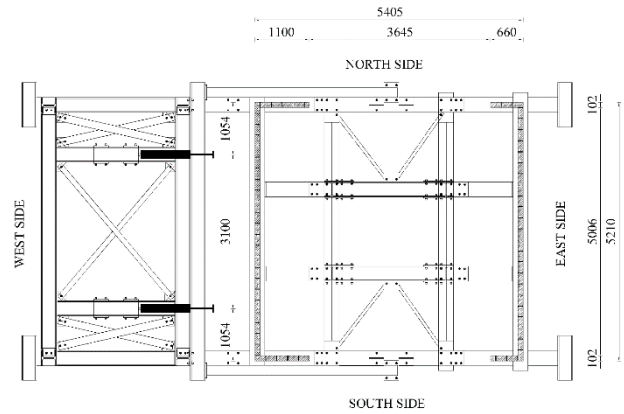
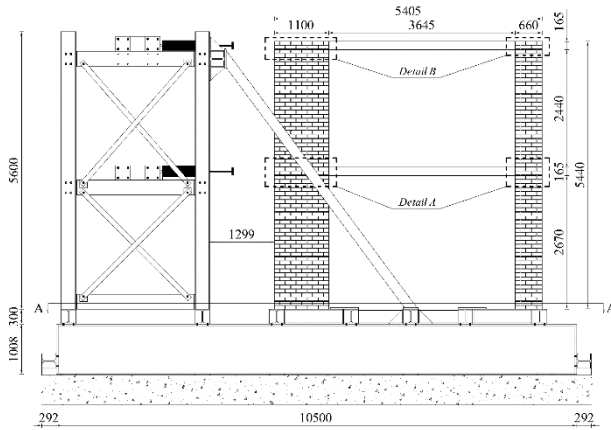
To provide a benchmark for the validation of analysis methods, the selected case study represents only the loadbearing parts of a typical terraced house. Figure 1 shows a 3D representation of the specimen and the test set-up. The facades of the specimens have a length of 5.4 m. Due to limitation of the set-up, the depth of the specimen was restricted to 5 m. The total height of the specimen is 5.4 m (Figure 2). The south and north facades, which are identically, are represented only by the slender piers connected to the transversal walls. Two sizes of the piers have been selected: on the western side the wide piers P1 and P3 have a width of 1.1 m, while on the eastern side the narrow piers P2 and P4 have a width of 0.6 m. The walls represent only the inner leaf of the cavity wall system and are made of calcium silicate brick masonry. The masonry was made in stretcher bond allowing for the interlocking of the bricks at the corners of the transversal walls and the piers (Figure 2b). Each floor consisted of two separated prefabricated concrete slabs spanning between the loadbearing transversal walls. The floors were laid up on the loadbearing walls in a mortar bed joint (Detail C in Figure 2d). The two separated concrete slabs per floor were then connected by cast-in-place reinforced concrete dowels, aiming to approach the behaviour of a monolithic floor. At the first floor level, the floor was connected horizontally to the piers by anchors of 6 mm diameter, cast in the floor and masoned in the piers (Detail A in Figure 2d). The narrow piers were connected by three anchors, while the wide piers by five anchors. These steel anchors are commonly used as horizontal buckling or wind load support of the pier, and they are not designed to withstand any vertical load. At the second floor level, the floor was laid on both the loadbearing walls and the piers. However, during construction the floor was first laid on the loadbearing transversal walls (Detail D in Figure 2d). Only after hardening of the mortar joint between the floor and the transversal walls, the joints between the floor and the piers were filled by mortar (Detail B in Figure 2d). Consequently, the weight of the floor is not directly carried by the piers in the facades, but only by the transversal walls.

Since the focus of the test is on the structural response, the specimen has been built on a rigid base foundation. The rigid base is mainly composed by two steel HEM 1000 beams positioned on the southern and northern side supported by the laboratory reinforced concrete floor (with thickness of 600 mm). These beams have been used as a base for a rectangular structure composed of HEB300 beams, which formed the foundation beams of the specimen. The first layer of the masonry walls was glued to the steel beams to avoid sliding at the base.

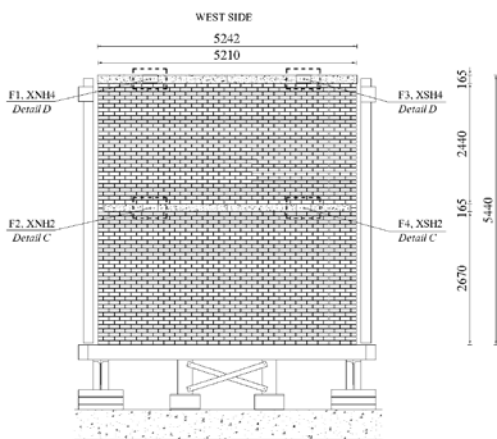
In order to apply the loading on the specimen, a braced steel tower was built (the blue steel structure in Figure 1, Figure 2). The tower, similarly to the specimen, was connected to the foundation beams. Because masonry shows very limited deformations in the elastic phase, it was aimed to limit the deformation of the test frame too. Stiffness requirements were governing over strength requirements. To increase the stiffness of the tower, two steel diagonal square tubes were connected from the top of the steel tower to the foundation beams. During the test, the vertical translation between the foundation beams and the laboratory floor were measured with linear potentiometers on several positions over the length of the beam, to evaluate the rotation of the specimen and of the tower. Measurements showed that these translations in Z direction and the accompanying rotations were negligible.



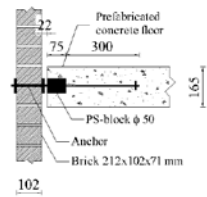
(a) (b)
Figure 1 – Set-up and test specimen: (a) 3D representation, (b) Picture.



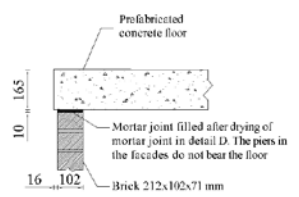
(a) (b)



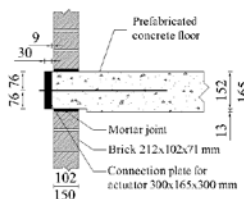
Detail A - First floor, facades



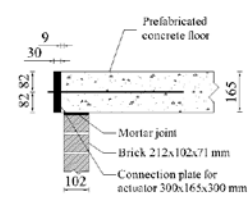
Detail B - Second floor, facades



Detail C - First floor, west side



Detail D - Second floor, west side



(c) (d)

Figure 2 – Set-up and test specimen: (a) Front view (southern side); (b) Top view of ground floor in section A-A; (c) Side view (western side); (d) Construction details.



3 Material properties

The material properties of masonry were selected to represent typical URM buildings of the period 1960-1980. This data were determined in a previous experimental campaign, in which masonry samples were extracted from existing building and tested in laboratory [17].

The replicated masonry adopted in the teste specimen was composed of calcium silicate bricks and general purpose mortar. The bricks had a nominal dimension of 210x71x102 mm and a nominal compressive strength of 16 MPa. A cement-based mortar in the M5 strength class was used. For both bricks and mortar a single batch of production was used. The thickness of both head and bed joints was set to 10 mm with possible variation between 9 to 12 mm. A strecher bond was selected.

A dedicated experimental campaign was performed for the characterisation of the replicated masonry [11]. Table 1 lists the obtained material properties. The compressive behaviour of masonry was determined both in the direction perpendicular and parallel to the bed joint following EN 1052-1 [18]. The masonry showed an orthotropic behaviour having a compressive strength higher in the direction perpendicular to the bed joint. The elastic modulus was approximatively the same in the two directions. The bending behaviour of masonry was determined in agreement with EN 1052-2 [19]. The flexural strength perpendicular to the bed joint resulted 4 times higher than the one parallel to the bed joints. The bond wrench test, performed in agreement with EN 1052-5 [20], showed bond strength value of 0.28 MPa, similar to the flexural strength parallel to the bed joint. Shear-compression tests on triplets were performed in agreement with EN 1052-3 [21] and the shear properties were derived following the Coulomb friction criterion. The masonry showed an initial shear strength of 0.14 MPa and a friction coefficient of 0.43.

To characterise the friction behaviour of the wall-to-floor connection, a shear-compression test was performed similarly to the one for masonry. Being the floor laying on the loadbearing walls and connected by a mortar joint, the friction behaviour is of importance. Applying the Coulomb friction criterion, the friction properties of the floor-to-wall connection resulted similar to the shear properties of masonry. Consequently, this connection can be considered equivalent to any other mortar joint.

Table 1 – Material properties of replicated calcium silicate brick masonry.

| Material property | Symbol | Unit | Average | Standard deviation |
|--|-------------|------|---------|--------------------|
| Compressive strength of masonry perpendicular to the bed joints | f_m^* | MPa | 5.8 | 0.5 |
| Compressive strength of masonry parallel to the bed joints | $f_{m,h}^*$ | MPa | 7.5 | 0.2 |
| Elastic modulus of masonry in the direction perpendicular to bed joints evaluated between 1/10 and 1/3 of the maximum compressive stress | E | MPa | 2887 | 460 |
| Elastic modulus of masonry in the direction parallel to the bed joints evaluated between 1/10 and 1/3 of the maximum compressive stress | E_h | MPa | 2081 | 864 |
| Out-of-plane masonry flexural strength parallel with the bed joint | $f_{x,1}$ | MPa | 0.21 | 0.05 |
| Out-of-plane masonry flexural strength perpendicular to the bed joint | $f_{x,2}$ | MPa | 0.76 | 0.36 |
| Flexural bond strength | f_w | MPa | 0.28 | 0.10 |
| Masonry initial shear strength of calcium silicate masonry | f_{v0} | MPa | 0.14 | - |
| Masonry shear friction coefficient of calcium silicate masonry | μ | - | 0.43 | - |
| Initial shear strength of bed joint between concrete floor and calcium silicate masonry | f_{v0}^* | MPa | 0.09 | - |
| Shear friction coefficient of bed joint between concrete floor and calcium silicate masonry | μ^* | - | 0.52 | - |
| Cubic compressive strength of concrete | f_{cc} | MPa | 74.7 | 1.7 |

4 Testing procedure

A quasi-static cyclic pushover test was performed on the assembled structure. The test was performed in displacement control with the additional condition of maintaining a constant ratio between the forces at the two floor levels. A ratio 1:1 between the forces was applied.

The masonry structure was loaded by four actuators, two per each floor. The actuators were positioned at approximately 1.1 meter inwards from the facades (Figure 2b). At the second floor level, the actuators No. 1 and 3 introduced a quasi-static cyclic horizontal deformation (Figure 2c). To impose a constant ratio between the forces at the two floor levels, the forces in the actuators No. 1 and 3 at the second floor level were mechanically coupled to the forces at the first floor level, by coupling the hydraulic system over the two floors, imposing that:

$$\begin{cases} F_1 = F_3 & \text{on the North side} \\ F_2 = F_4 & \text{on the South side} \end{cases} \quad (1)$$

The displacements at the second floor level were imposed in 21 cycles; each of them composed by 3 runs (Figure 3). A run is defined as the time needed to apply the maximum positive and negative target displacement starting and ending at zero. The speed of the imposed horizontal deformations was chosen for every cycle such that the cycle lasted 15 minutes. As a result of the increasing amplitude, the constant cycle time resulted in a deformation velocity increasing per cycle. Table 2 lists the maximum and minimum average displacement imposed at the second floor level d_2 for every cycle.

The deformation of the specimen was measured in absolute sense from a stiff wooden frame, which was connected neither to the tower nor to the foundation beams. The displacements along the X-axis, at the point of application of the loading, have been measured with draw wires with length of 150 mm.

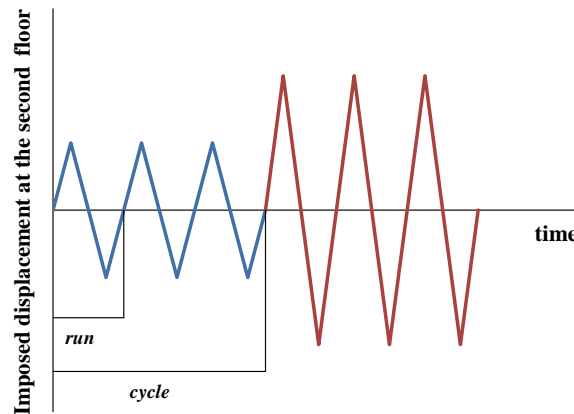


Figure 3 – Loading scheme.

Table 2 – Applied target displacements for every cycle in initial, pre- and post-peak phase.

| | Cycle | $d_{2,min}$ | $d_{2,max}$ | | Cycle | $d_{2,min}$ | $d_{2,max}$ | | Cycle | $d_{2,min}$ | $d_{2,max}$ |
|----------------------|-------|-------------|-------------|-----------------------|-------|-------------|-------------|------------------------|-------|-------------|-------------|
| | | mm | mm | | | mm | mm | | | mm | mm |
| Initial phase | 1 | -0.31 | 0.25 | Pre-peak phase | 9 | -3.40 | 3.17 | Post-peak phase | 15 | -21.30 | 22.16 |
| | 2 | -0.70 | 0.61 | | 10 | -4.38 | 4.13 | | 16 | -26.89 | 27.91 |
| | 3 | -1.14 | 0.94 | | 11 | -6.01 | 5.80 | | 17 | -38.15 | 39.13 |
| | 4 | -1.57 | 1.33 | | 12 | -9.07 | 8.96 | | 18 | -49.31 | 50.62 |
| | 5 | -2.01 | 1.73 | | 13 | -12.24 | 12.16 | | 19 | -60.13 | 61.82 |
| | 6 | -2.45 | 2.14 | | 14 | -15.49 | 15.43 | | 20 | -70.97 | 73.04 |
| | 7 | -2.89 | 2.58 | | | | | | 21 | -82.31 | 84.23 |
| | 8 | -3.36 | 3.01 | | | | | | | | |



5 Experimental results

The pushover test was performed in three phases named initial, pre-peak and post-peak phase. For each phase a visual inspection of the specimen was carried out after every cycle to identify the development of the crack pattern. In this section, the results in terms of capacity curve, crack pattern and drift of the two floors are reported.

Figure 4 shows the capacity curve of the assembled structure together with the corresponding backbone curve. Due to the different pier lengths, the behaviour in capacity and ductility results are asymmetric. This asymmetric behaviour results directly correlated to the crack pattern evolution (Figure 6).

The initial phase consisted of the first 8 cycles, in which a maximum displacement of $d_2 = \pm 3.0$ mm is reached. In this phase, the structure primarily shows a linear elastic behaviour. By analysing the capacity curve, the initial stiffness of the building could be estimated up to 15.6 kN/mm. In this phase, horizontal cracks with a maximum opening of approximately 1 mm were measured by the sensors (Figure 5), but they could not be recorded by the visual inspection (Figure 6). Figure 5 shows the development of these cracks for the corner between the western wall and the pier P1; a similar behaviour was observed in the other corners. The horizontal cracks were located at the interface between the floor and the transversal walls and at the bottom of the piers (Figure 5). For both the western and eastern transversal walls (Figure 5a, b), the cracks were wider at the corner rather than at the centre of the wall. The wider cracks were measured at the second floor level, while at the first floor level an opening of maximum 0.1 mm was recorded. At the ground floor level, the opening was negligible both at the centre and on the south corner of the transversal walls. For both the western (P1 and P3) and the eastern (P2 and P4) piers the maximum crack opening was measured at the bottom free side of the pier (Figure 5c, d). Due to the different size of the piers, a larger opening was recorded for the western piers (P1 and P3). Due to these horizontal cracks, a reduction of the stiffness in the negative direction (from eastern to western side) was observed in the capacity curve in correspondence of cycle 7 ($d_2 = \pm 2.7$ mm).

In the pre-peak phase, cycle 9 to 14 were executed to reach a maximum displacement of $d_2 = \pm 15.5$ mm. In this phase, all the piers visibly showed the horizontal cracks at both bottom and top side, which were previously measured in the initial phase. The cracks in correspondence of the ground floor level developed within the first mortar joint, being the masonry glued on the foundation beams. Extensive horizontal cracks developed also in the transversal walls: for the western wall, they were mainly concentrated at the ground floor level, while for the eastern wall they were located at the second floor level. In this phase, the first diagonal cracks occurred on the transversal walls. They were mainly located at the ground floor on the western side.

In the post-peak phase, cycle 15 to 21 were executed to reach a maximum displacement of $d_2 = \pm 82.0$ mm. The structure presented an asymmetrical behaviour for loading in the positive (from west to east side) and negative (from east to west side) direction. The maximum capacity was first reached for positive displacements. During cycle 15 ($d_2 = \pm 21.8$ mm), the maximum base shear force of 47.3 kN was reached for positive displacement, while for negative displacement approximately 97% of the maximum capacity was reached. During this cycle, the previously observed horizontal and diagonal crack on the transversal walls further extended. After the peak, the capacity and stiffness substantially reduced for positive displacements. This phenomenon was mainly governed by the diagonal/vertical cracks occurring first in pier P3 and subsequently in pier P1. Due to the extensive cracking of these piers, part of pier P3 was removed for safety reasons after cycle 19. For negative displacements, the maximum base shear force of 41.6 kN was reached in correspondence of a displacement of -60 mm (cycle 19). This event corresponded to the formation of a secondary diagonal/vertical crack in pier P3. During the post-peak phase, the out-of-plane crack on the transversal walls further developed, by forming the typical yield line envelope. In the last two cycles, where a maximum displacement of ± 82 mm was reached, the out-of-plane cracks became dominant on the eastern wall.

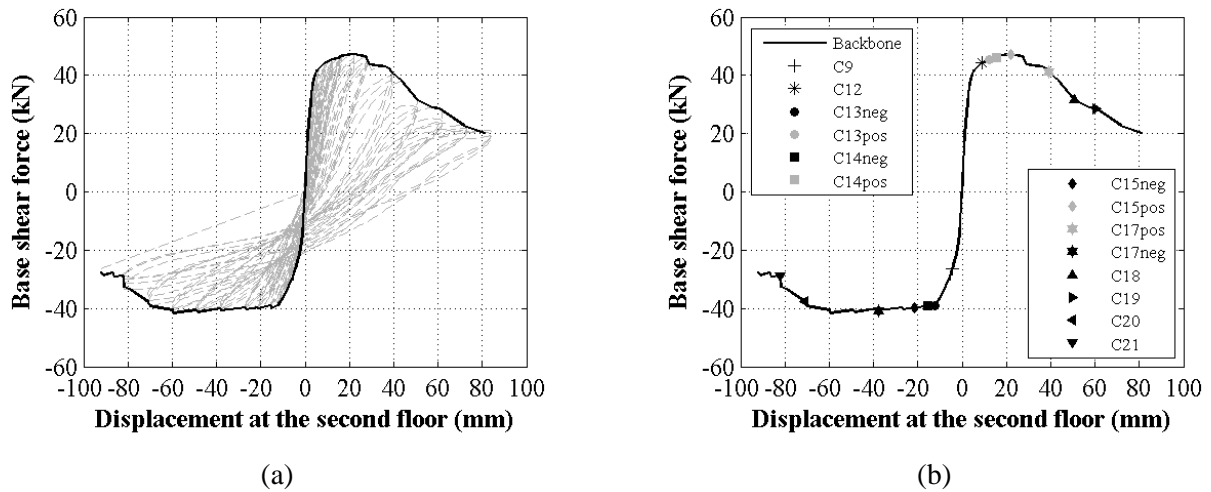


Figure 4 – Response of the assembled structure: (a) Capacity curve and corresponding backbone curve; (b) Cycle in correspondence of cracking observations (see also Figure 6)

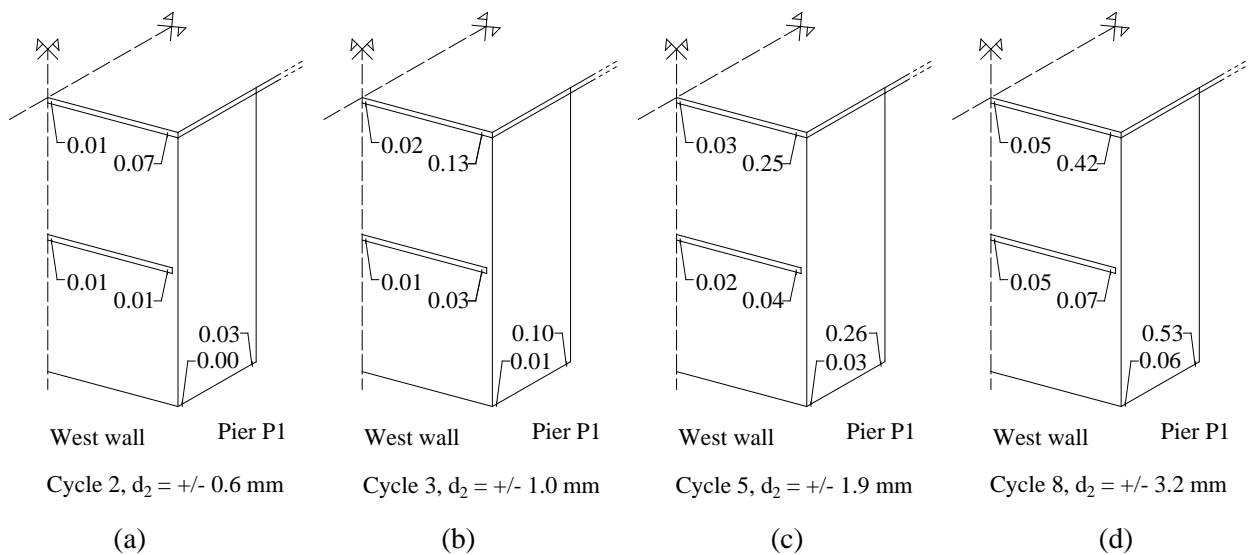


Figure 5 – Maximum opening of horizontal cracks at the floor-to-wall connection (western wall) and at the bottom of the pier P1, measured on the outside of the specimen during the initial phase (unit: mm).

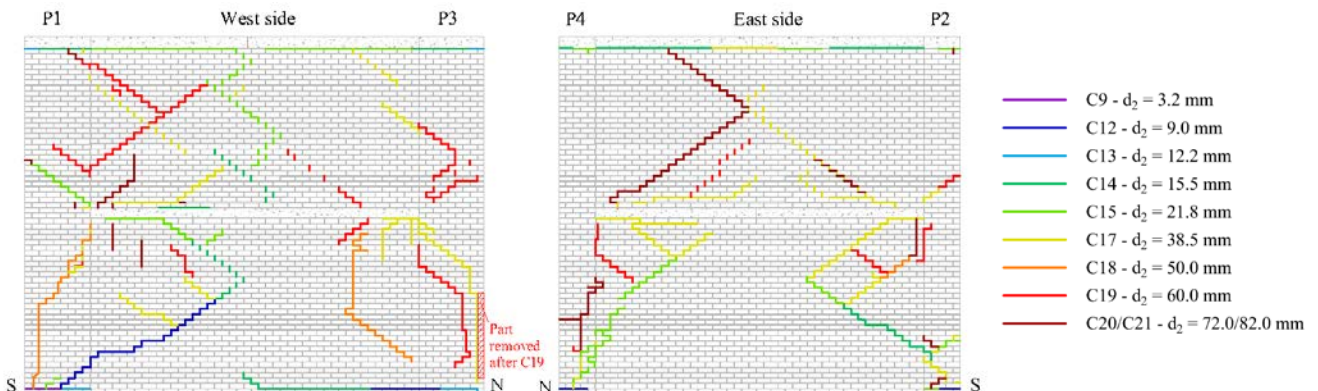
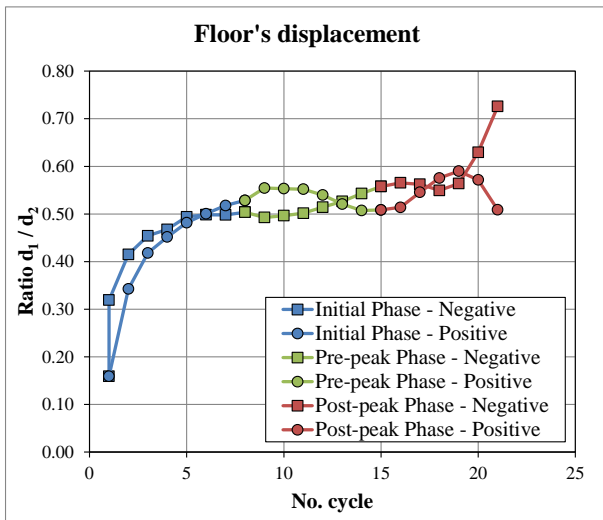


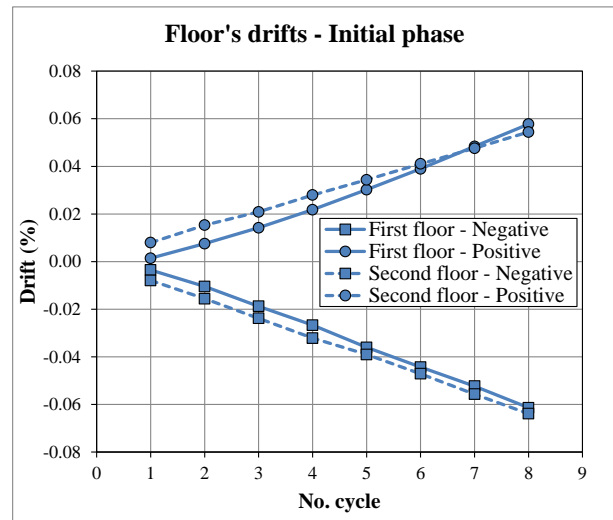
Figure 6 – Crack pattern defined on the base of visual inspection (see also Figure 4).

Figure 7a reports the behaviour of the structure in terms of floor displacements. The ratio of the floors' displacement was ranging between 0.2 and 0.5 in the initial phase; afterwards a constant trend was observed in the pre- and post-peak phases. Similar values of the ratio between the floor's displacements were observed for the loading in the positive and negative direction, with the exception of the last two cycles. In these cycles, the first floor level showed larger displacement for negative loading than for positive loading. This can be correlated to the opening/closing mechanism interesting the cracks in the western piers. These cracks are only located at the ground floor level and they interest also the connection of the piers with the transversal walls. If the specimen is subjected to negative displacements, these cracks are open and allow for large displacement of the transversal walls, thus of the first floor level. On the contrary, if positive displacement is applied to the specimen, these cracks are closed limiting the displacement of the floor.

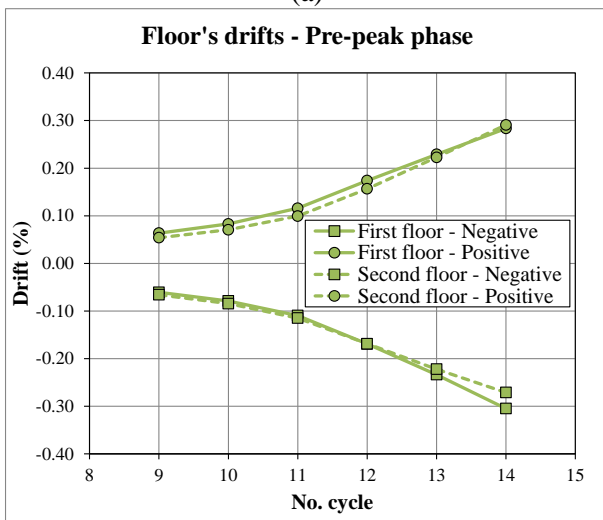
Figure 7b-d reports the behaviour of the structure in terms of drifts. They are calculated as the ratio between the relative floor displacement and the interstorey height, which is 2.7 and 2.6 m for the first and second floor level, respectively. In the initial and pre-peak phase, both the first and second floor show similar drift values. At the end of the post-peak phase, a difference is observed, for both floor levels, between the drifts values obtained for negative and positive loading. This difference can be correlated to the extensive damage within the western piers. A maximum drift of +1.6/-2.4 % was reached at the first floor level, while the second floor showed a drift of +1.6/-1.0 %.



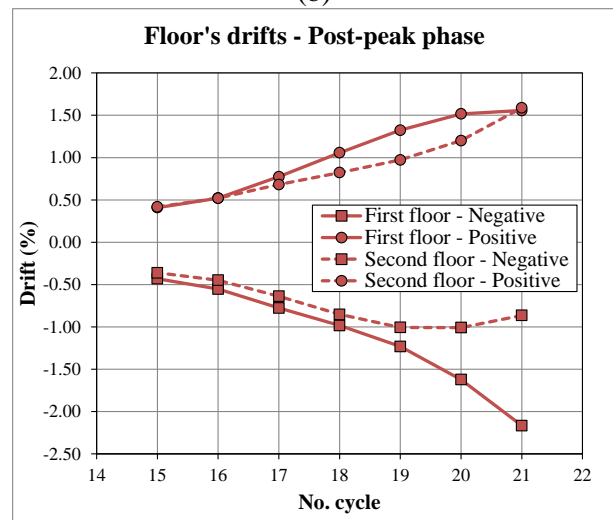
(a)



(b)



(c)



(d)

Figure 7 – (a) Ratio between first and second floor displacement; (b)-(d) Drifts of first and second floor (calculated with $H_{1st\ floor} = 2753\ mm$, $H_{2nd\ floor} = 2605\ mm$)



6 Analytical estimation

In order to qualitatively explain the pre-peak behaviour of the assembled structure, an analytical estimate is presented in this section based on the observed damage evolution. The formation of the horizontal cracks at the floor-to-wall connections and at the piers edges is considered. In these calculations, the material properties of the masonry presented in Section 4 are adopted; the density of the masonry and of the concrete are respectively assumed equal to 2000 and 2400 kg/m³.

To represent the elastic phase of the test, a portal schematization is considered (Figure 8b). In this phase, the wall-to-floor connection is considered as a moment resisting connection. The masonry walls are represented as C-shaped elements to account for the flange effect. Accordingly to Ref. [2], the western (P1, P3) and eastern (P2, P4) piers can activate, through the flange effect, a contributing length of the transversal walls equal to 1300 mm (Figure 8a). The analytical calculation estimates an elastic capacity of approximately 10 kN and an initial stiffness of 21.7 kN/mm. Experimentally a similar elastic capacity and an initial stiffness of 15.1 kN/mm were measured.

To represent the pre-peak phase of the test, two assumptions are made: 1) it is conservatively assumed that the horizontal cracks at the floor-to-wall connection are developed for the entire length of the wall; 2) it is considered that the capacity of the structure is governed by the behaviour of the piers. The second hypothesis is also supported by the large-scale experimental tests on walls subjected to two-way out-of-plane bending. These tests showed that the walls could withstand displacements up to 90% of their thickness (more details can be found in Refs. [13]-[14]). Considering the first assumption, the degraded stiffness is evaluated with the previously adopted portal schematization, which is modified considering hinged connections between the transversal walls and the floors (Figure 8c). The analytical calculation provides a degraded stiffness of 5.8 kN/mm. Considering the second assumption, the capacity of the structure is calculated from the force equilibrium in the piers assuming that only horizontal forces can be transferred between them, as shown in Figure 9. The piers are subject to vertical forces due to the weight of the floors, of transversal walls and their own weight. It is assumed that the entire weight of the floor is transferred to the piers in an equal manner. Due to the horizontal cracking at the floor-to-wall interface, the normal force due to the second floor changes its position on the base of the applied horizontal loading direction, thus of the vertical movement of the piers. Considering the effect of the wall-to-pier interlocked connection and the initial crack pattern, a trapezoidal part of the transversal wall is assumed cooperating with the piers [2] (Figure 9a). Considering the piers equilibrium, the estimated capacity results approximately equal to 49 and -42 kN for the positive and negative direction, respectively. Considering the estimates of the degraded stiffness and capacity, an extrapolation of the analytical calculation can be made in the pre-peak phase (Figure 10).

The analytical calculation is able to qualitatively capture the pre-peak behaviour of the structure and estimate its capacity (Figure 10). Even if this estimation is adopted only for a qualitative comparison, some relevant conclusions can be drawn: 1) the connection between floor and wall is of importance with respect to the elastic behaviour of the specimen in terms of both stiffness and capacity; 2) the entire weight of the floor is activated during the test; 3) the maximum base shear force of the structure directly depends on the maximum in-plane capacity of the piers.

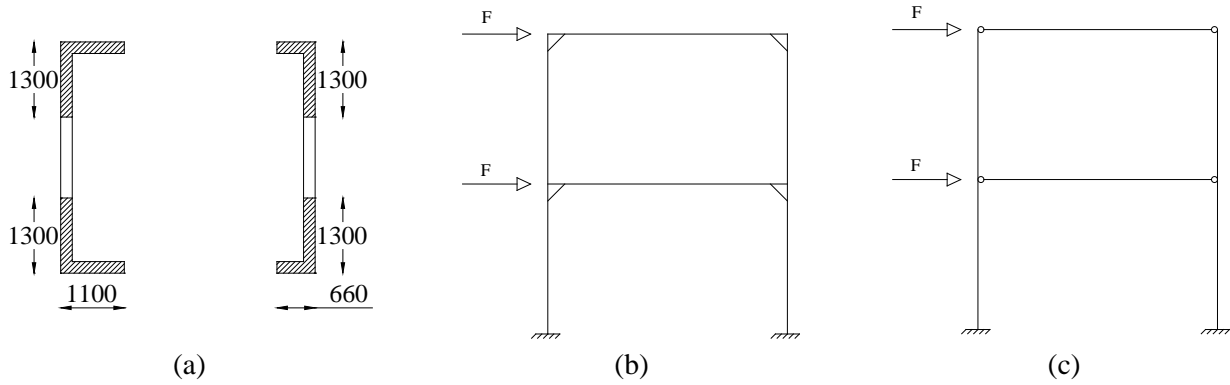


Figure 8 – Portal schematization to represent the: (a) Effective cross section; (b) Scheme with moment resisting connections to represent the elastic phase; (c) Scheme with hinged connections to calculate the reduced stiffness in the pre- and post-peak phase.

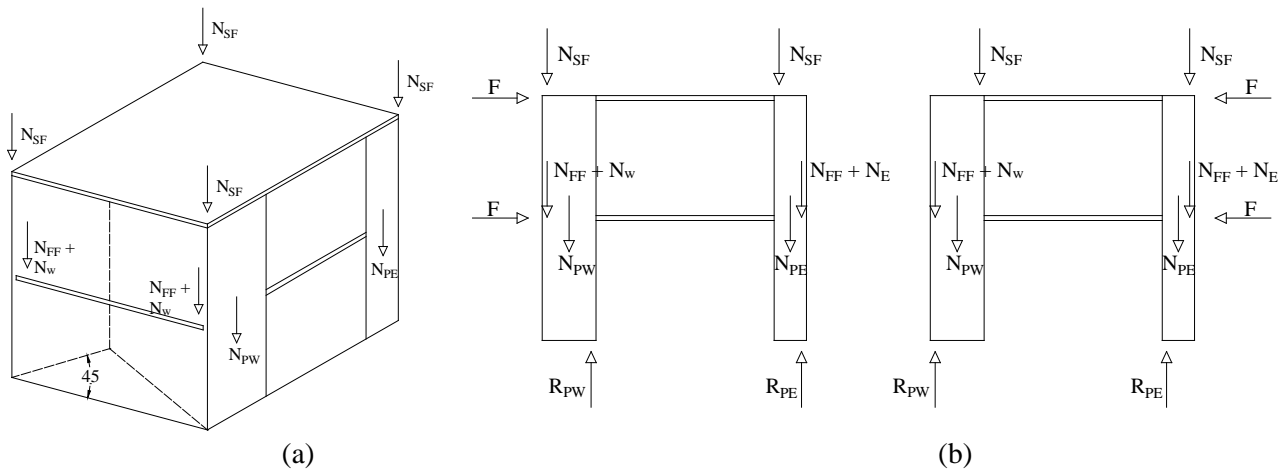


Figure 9 – Schematization adopted in the analytical estimate of the capacity: (a) Volume partition of the floors and of the transversal walls loading the piers; (b) Forces loading the piers for positive and negative loading.

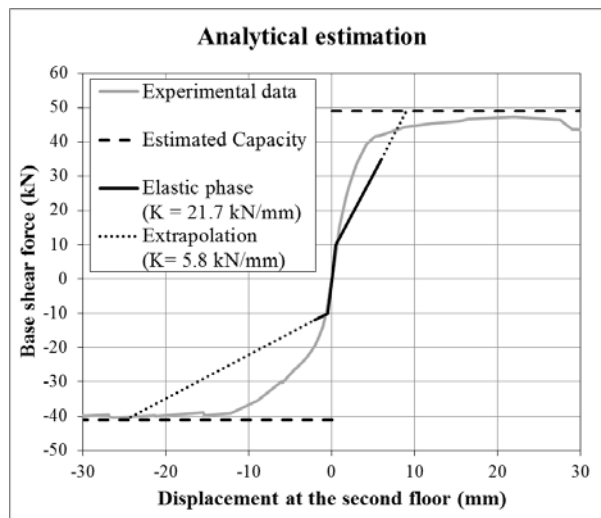


Figure 10 – Comparison between experimental results and analytical calculation.



7 Concluding remarks

Due to the increase of the seismicity activity in the north part of the Netherlands, the assessment of unreinforced masonry structures is of importance. These structures, which represent the majority of the residential buildings in the area, are not designed according to seismic resistance rules.

In order to study the response of URM buildings, a cyclic pushover test on a full-scale two-story high building was carried out at Delft University of Technology. The selected case study resembled a typical Dutch terraced house built between 1960 and 1980, although some simplifications were made for clarity sake. The tested specimen represents only the loadbearing part of the selected case study and it is characterised by slender walls in calcium silicate masonry and prefabricated concrete floor. The specimen was tested under cyclic loading imposing the displacement at the second floor level and ensuring that the ratio between the forces at the two floor levels was equal to 1.

Analysing the evolution of the damage in the structure and adopting a qualitative analytical calculation, it could be concluded that the behaviour of the structure was mainly governed by the in-plane behaviour of the piers. Being the western and eastern piers different in sizes, an asymmetrical behaviour was observed both in terms of maximum base shear force and hysteretic behaviour. Due to the running bond between the transversal walls and the piers, the former were subjected to two-way out-of-plane bending and they were thus able to withstand large deformation.

In conclusion, the performed experimental tests result a unique benchmark for the Dutch situation, where particular building characteristics and recent seismic activity increased the need of validation of analysis methods for the assessment.

Acknowledgements

This research was funded by Nederlandse Aardolie Maatschappij B.V. (NAM) under contract number UI46268 “Physical testing and modelling – Masonry structures Groningen”, which is gratefully acknowledged, and developed in cooperation with the engineering company ARUP and the European Centre for Training and Research in Earthquake (EUCentre).

References

- [1] Benedetti, D, Carydis, P, and Pezzoli, P (1998): Shaking table tests on 24 simple masonry buildings. *Earthquake Engineering & Structural Dynamics*, **27**(1), 67-90.
- [2] Yi, T. (2004): Experimental investigation and numerical simulation of an unreinforced masonry structure with flexible diaphragms. Ph.D. thesis. Georgia Institute of Technology.
- [3] Magenes, G, Kingsley, G R and Calvi, GM (1995): Seismic testing of a full-scale, two-story masonry building: test procedure and measured experimental response. Consiglio nazionale delle ricerche, Gruppo nazionale per la difesa dai terremoti.
- [4] Raijmakers TMJ, Vermeltfoort AT (1992): Deformation controlled meso shear tests on masonry piers. Report B-92-1156, TNO-BOUW/TU Eindhoven, Eindhoven, The Netherlands.
- [5] Anthoine A, Magonette G, Magenes G (1995): Shear-compression testing and analysis of brick masonry walls. Proceedings of the 10th European conference on earthquake engineering, Vienna, Austria.
- [6] Tomazevic M, Lutman M, Petkovic L (1996): Seismic behavior of masonry walls: experimental simulation. *Journal of Structural Engineering*, **122**(9), 1040-1047.
- [7] Derakhshan H, Griffith MC, Ingham JM (2011): Out-of-plane behavior of one-way spanning unreinforced masonry walls. *Journal of Engineering Mechanics*, **139**(4), 409-417.
- [8] Griffith MC, Vaculik J, Lam NTK, Wilson J, Lumantarna E (2007): Cyclic testing of unreinforced masonry walls in two-way bending. *Earthquake Engineering & Structural Dynamics*, **36**(6), 801-821.
- [9] Doherty, K, Griffith, MC, Lam, N, & Wilson, J (2002): Displacement-based seismic analysis for out-of-plane bending of unreinforced masonry walls. *Earthquake Engineering & Structural Dynamics*, **31**(4), 833-850.
- [10] Mariani V, Messali F, Hendriks MAN, Rots JG (2017) Numerical modelling and seismic analysis of Dutch masonry structural components and buildings, *16th World Conference on Earthquake Engineering, 16WCEE 2017*, Santiago, Chile.



- [11]Esposito R, Messali F and Rots JG, (2016): Material characterisation of replicated masonry and wall ties. Delft University of Technology. *Final report 18 April 2016*.
- [12]Ravenshorst G and Messali F (2016): In-plane tests on replicated masonry walls. Delft University of Technology. *Final report 18 April 2016*.
- [13]Ravenshorst G and Messali F (2016): Out-of-plane test on replicated masonry walls. Delft University of Technology. *Final report 29 April 2016*.
- [14]Messali F, Ravenshorst G, Esposito R and Rots JG (2017): Large-scale testing program for the seismic characterization of Dutch masonry structures. *16th World Conference on Earthquake, 16WCEE 2017*, Santiago, Chile.
- [15]Ravenshorst G, Esposito R, Schipper R (2016): Quasi-static cyclic pushover test on the assembled masonry structure at TU Delft. Delft University of Technology. Preliminary report 3 February 2016.
- [16]Graziotti F, Tomassetti U, Rossi A, Kallioras S, Mandirola M, Penna A and Magenes G (2015): Experimental campaign on cavity walls systems representative of the Groningen building stock. *Report EUC318/2015U*, Eucentre, Pavia, Italy.
- [17]Jafari S, Panoutsopoulou L and Rots JG (2015): Tests for the characterisation of original Groningen masonry. Delft University of Technology. Final report 18 December 2015.
- [18]EN 1052-1 (1998): Method of test masonry – Part 1: Determination of compressive strength. *Nederlands Normalisatie-instituut (NEN)*.
- [19]EN 1052-2 (1999): Method of test masonry – Part 2: Determination of flexural strength. *Nederlands Normalisatie-instituut (NEN)*.
- [20]EN 1052-5 (2005): Method of test masonry – Part 5: Determination of bond strength by bond wrench method. *Nederlands Normalisatie-instituut (NEN)*.
- [21]EN 1052-3 (2002): Method of test masonry – Part 3: Determination of initial shear strength. *Nederlands Normalisatie-instituut (NEN)*.